A Tunable Dual-Band Miniaturized Monopole Antenna for Compact Wireless Devices

Raoul O. Ouedraogo, *Member, IEEE*, Junyan Tang, *Student Member, IEEE*, Kazuko Fuchi, Edward J. Rothwell, *Fellow, IEEE*, Alejandro R. Diaz, and Prem Chahal, *Member, IEEE*

***Abstract*—A technique for producing miniaturized tunable planar monopole antennas for wireless communication applications is introduced. Miniaturization is achieved by optimizing the geometry of a pixelated metallic patch surrounding the monopole antenna. Tuning of the antenna is implemented by varying the capacitance of a varactor diode loaded between the pixelated metallic patch and the ground plane. The result is an ultra-compact, dual band, folded monopole antenna that fits into a hemisphere of radius $\lambda_0/20$ at 2.1 GHz. Varying the capacitance of the varactor diode enables the two resonance frequencies to be tuned simultaneously, covering multiple frequency bands for different wireless applications. A prototype antenna has been fabricated and measured, confirming the feasibility of the proposed design.**

***Index Terms*—Broadband antennas, genetic algorithms, miniaturization, tunable circuits and devices, varactors, wireless communication.**

I. Introduction

THE RECENT upsurge in demand for compact mobile devices has driven innovations in the interoperability of devices and applications. In particular, new methods for designing compact, multiband antennas at low manufacturing cost are being emphasized by device manufacturers.

The physical dimensions of antennas can be miniaturized through various techniques including the use of high-permittivity dielectrics, meander lines, fractals, and shorting pins [1]–[3]. Combinations of several miniaturization techniques can also be used to produce even smaller antennas. An example is an element such as a meander line or a shorted monopole encapsulated in a high-dielectric-constant material such as ceramic or silicon [4]–[6]. Antenna miniaturization can also be achieved through metamaterial loading. Ouedraogo *et al.* show that the resonance frequency of a loop antenna can be reduced by placing an optimized double-sided pixelated patch above the loop [7].

One of the consequences of antenna miniaturization is a reduction in bandwidth, which imposes severe limitations on the practical use of the antenna. This can be alleviated in some applications by implementing a frequency tuning system, several variants of which have been devised. For instance, it is shown in [8] that by placing computer controlled switches between a patch antenna and its ground plane, the resonance frequency of the antenna can be varied by turning the switches on and off. However, to achieve an adequate tunable bandwidth, a high number of switches or micro-actuated pixels is often required, increasing the complexity and cost of fabrication and implementation. Varactors provide an alternative and appealing means for tuning [10], [11]. Since the capacitance of the varactor varies with the supplied dc bias voltage, the resonance frequency of the antenna can be tuned continuously.

Many antennas have the additional requirement that they must operate simultaneously within multiple bands, while maintaining the ability to tune within each band. In [12], it is shown that the operating band of a multiple-input–multiple-output (MIMO) antenna can be reconfigured by switching the states of p-i-n diodes, while frequency tuning within the band is accomplished by changing the length of coupled conductors. Alternatively, [13] and [14] have shown that multiband tuning can be achieved by loading varactor diodes on a multiresonance structure, such as a multibranch monopole or a planar inverted-F antenna (PIFA). However, these antennas suffer either from a large profile or a limited tuning range and are not optimal for applications where wireless devices are required to be highly compact and multifunctional.

In this letter, the pixelated antenna optimization approach described in [7] is used in combination with varactor loading to produce a miniaturized, tunable, monopole antenna suitable for small integrated device applications. A novel optimization approach is proposed in which the capacitance of the varactor is included during optimization, as opposed to adding a tuning component to an already optimized structure. This greatly improves the tunable bandwidth of the final design and eliminates the lengthy experimentation normally required to determine the characteristics and appropriate placement of a tuning element.

The proposed antenna, which can fit into a hemisphere of radius $\lambda_0/20$ at 2.1 GHz, has two operating bands: 2.2–2.6 and 3–4.2 GHz. These cover the WLAN band of 2.4–2.48 GHz; the WiMAX frequency bands of 3.3–3.4, 3.4–3.6, and 3.6–3.8 GHz; and the 3.6-GHz WLAN band (802.11y). To minimize the overall size of the antenna, the biasing circuit is integrated into the area of the pixelated antenna structure. Taken together, these features provide a novel antenna in that a significant reduction of complexity and size is coupled with a wide tuning

Manuscript received April 09, 2014; revised May 27, 2014; accepted June 17, 2014. Date of publication June 24, 2014; date of current version July 10, 2014.

R. O. Ouedraogo, J. Tang, E. J. Rothwell, and P. Chahal are with the Department of Electrical and Computer Engineering, Michigan State University, East Lansing, MI 48824 USA (e-mail: rothwell@egr.msu.edu).

K. Fuchi and A. R. Diaz are with the Department of Mechanical Engineering, Michigan State University, East Lansing, MI 48824 USA (e-mail: diaz@egr.msu.edu).

Color versions of one or more of the figures in this letter are available online at http://ieeexplore.ieee.org.

Digital Object Identifier 10.1109/LAWP.2014.2332752

1536-1225 © 2014 IEEE. Personal use is permitted, but republication/redistribution requires IEEE permission.
See http://www.ieee.org/publications_standards/publications/rights/index.html for more information.
Authorized licensed use limited to: JAMES MALONEY. Downloaded on February 19,2026 at 15:48:23 UTC from IEEE Xplore. Restrictions apply.

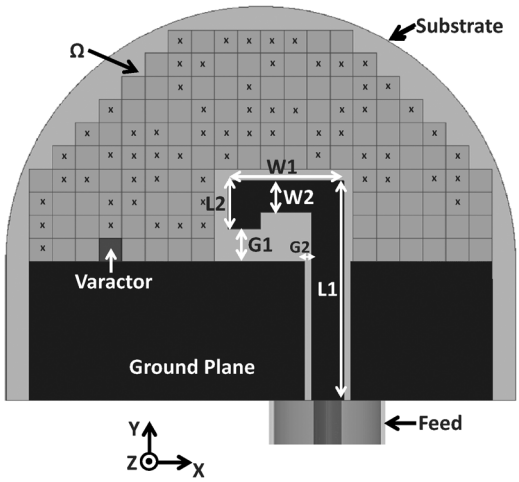

Fig. 1. Front view of the monopole antenna inscribed in a pixelated half-disk. Crosses indicate the "on" pixels of the optimized antenna.

range over a dual band. Details of the design and results from both simulation and measurement are provided as follows.

II. Design

The pixelization approach presented in [7] is used here to create a miniaturized planar antenna on a thin, low-permittivity dielectric. A coplanar waveguide (CPW) is used to excite a small folded monopole antenna that is inscribed in a metallic patch placed above a small integrated ground plane as shown in Fig. 1. The CPW enables a convenient connection between the antenna and neighboring circuit components. The antenna and the patch are backed by a thin dielectric substrate, and the back side of the substrate is coated with copper except for a 1.8-mm-wide strip to provide isolation from the attached coaxial cable. The purpose of the copper backing is to provide shielding of the antenna from neighboring electronics when integrated into a compact wireless device, and not to provide a return path for the CPW.

The metallic patch, which is used as a parasitic loading element, is parameterized as a pixelated grid. Turning the pixels of the grid on or off alters the electrical characteristics of the patch, thus affecting the performance of the antenna. The total number of pixel configurations is 2^n where n is the number of pixels composing the patch. In this letter, the patch is parameterized into 134 pixels leading to a total of 2^{134} possible pixel configurations. The large number of pixel configurations suggests the use of a binary optimizer capable of quickly finding pixel configurations that produce acceptable performance.

The goal of the design is to demonstrate frequency tuning by varying the capacitance of a varactor placed between the ground plane and the pixelated patch. Rather than optimizing the patch first and then adding the varactor, one of the pixels in direct contact with the ground plane is replaced by a fixed capacitor during optimization. By including the capacitance during the optimization process, the final design has a much wider tunable bandwidth. The position of the replaced pixel is not crucial, but a position about halfway between the monopole and the edge of the ground plane works well and provides the largest amount of space for mounting the varactor on the prototype antenna. The value of the fixed capacitor was set to 2 pF during optimization since it represents the largest capacitance of the varactor that was planned for the prototype. Optimizing with the largest value sets the lower edge of the tunable frequency band, and the resonance frequency can then be tuned upward after an acceptable structure has been finalized by decreasing the capacitance of the varactor.

The optimization procedure is based on the integration of the full-wave solver HFSS with a genetic algorithm (GA) written in MATLAB [7]. To perform the GA, the pixels of the grid are encoded into a binary string. Each combination of zeros and ones of the binary string corresponds to a specific pixel configuration or patch geometry. The GA is configured for a tournament selection with two crossover points and two mutation bits. An initial population of 200 different binary strings is selected randomly, and the associated geometries of the patch and antenna are created in MATLAB and exported to HFSS for simulation. The reflection coefficient $S_{11}^{(1,2)}$ and efficiency $\eta_r^{(1,2)}$ of the simulated antenna at the two target frequencies $f_{1,2}$ are exported back to MATLAB, and the fitness of each pixel configuration is evaluated using the fitness function

$$\text{fitness} = 50\left[\eta_r^{(1)} + \eta_r^{(2)}\right] - 20\log_{10}\left|S_{11}^{(1)}\right|\left|S_{11}^{(2)}\right|. \quad (1)$$

Once all the pixel configurations of the initial population have been evaluated, their fitnesses are calculated and ranked. The top 20% are selected for crossover and mutation until a new population of 200 binary strings is generated. This process is repeated until the maximum number of generations set to 20 is reached. Thus, maximizing this fitness function corresponds to finding pixel configurations that lead to high efficiencies and low reflection coefficients.

III. Simulations

To investigate the potential of the compact tunable monopole antenna, the geometry of a metallic patch shaped into a half-disk of radius 5.2 mm was optimized in close proximity to the monopole antenna to create a resonance at a frequency much lower than the initial resonance of the monopole antenna. The term *initial resonance* corresponds to the resonance of the monopole in absence of the pixelated patch. The half-disk is parameterized into 158 square pixels of side length 0.52 mm; 24 pixels located in the middle of the half-disk are turned off by default to allow enough space for the monopole. The dimensions of the monopole antenna are $W1 = 2.6$ mm, $W2 = 0.728$ mm, $L1 = 4.94$ mm, and $L2 = 1.092$ mm. The dimensions of the ground plane are 3.12×10.4 mm^2, and the gaps between the ground plane and the monopole antenna are $G1 = 0.728$ mm and $G2 = 0.15$ mm. The ground plane, monopole antenna, and the pixelated patch are backed by a 0.5-mm Rogers RO4003 substrate with a dielectric constant $\epsilon_r = 3.55$ and a loss tangent $\delta = 0.0027$. The initial resonance of the monopole antenna is at 5.4 GHz, and the goal of the optimization is to find a pixel configuration that creates resonances at 2.1 and 3.7 GHz. Note that at 2.1 GHz, the antenna fits into a hemisphere with a radius of 5.2 mm, or approximately $\lambda_0/20$, where λ_0 is the free-space wavelength. The GA optimization identified several structures resonating at 2.1 and 3.7 GHz with reflection coefficients of -15 dB or smaller. Of those, the structure producing the best combination of return loss and

Authorized licensed use limited to: JAMES MALONEY. Downloaded on February 19,2026 at 15:48:23 UTC from IEEE Xplore. Restrictions apply.

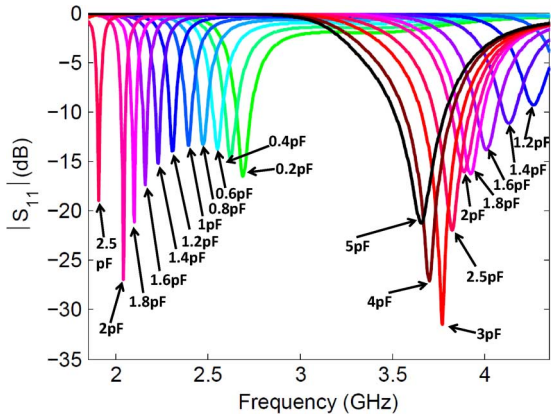

Fig. 2. Simulated reflection coefficients for various capacitance values.

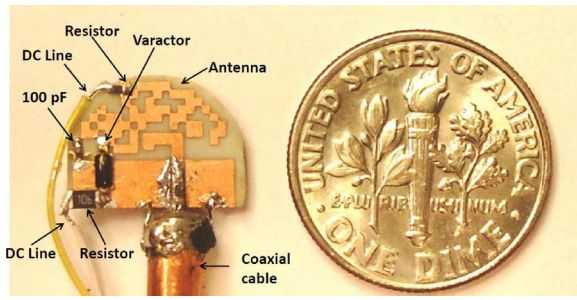

Fig. 3. Prototype miniature antenna next to a US dime (17.91 mm diameter).

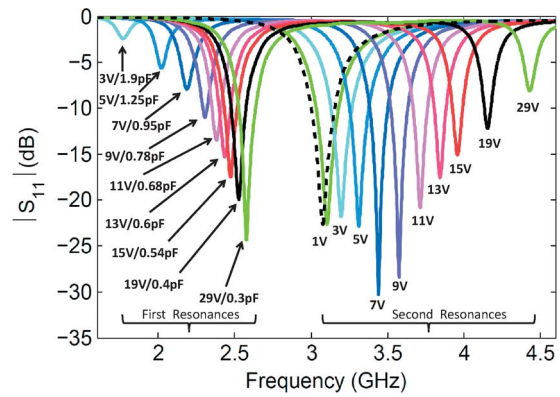

Fig. 4. Measured reflection coefficients for various varactor capacitances.

efficiency was chosen for fabrication. The pixels composing that structure are shown in Fig. 1.

To investigate the tunable frequency range of the optimized antenna, the capacitance originally fixed at 2 pF during optimization was varied from 0.2 to 5 pF with a step of 0.2 pF, and a full-wave analysis of the antenna using HFSS was performed for each capacitance. An ideal capacitance model was used in the simulations, and the capacitance range of 0.2–5 pF was selected to correspond to the range of the varactor diode used in subsequent measurements of a fabricated prototype.

Fig. 2 shows plots of the simulated reflection coefficient of the optimized antenna. Two resonances are clearly identified. As the capacitance is decreased (corresponding to an increase in a varactor voltage), the resonance frequencies move upward. For the lower resonance, reducing the capacitance from 2.5 to 0.2 pF shifts the frequency of resonance from 1.9 to 2.7 GHz, corresponding to a tuning range of 42.1% referenced to the lower band. For the upper resonance, the resonance frequency can be shifted from 3.7 to 4.2 GHz by varying the capacitance from 5 to 1.4 pF. Although the resonances can be shifted outside these bounds by increasing or decreasing the capacitance further, the results become less satisfactory in terms of return loss or efficiency.

IV. Prototype Measurements

A prototype was fabricated using the antenna structure corresponding to the highest fitness found during GA optimization (indicated in Fig. 1 by the pixels with crosses). All dimensions and substrate characteristics are the same as used in the simulations. A picture of the prototype is shown in Fig. 3. An Aeroflex MGV-100-25 hyperabrupt varactor diode was used to investigate the frequency tuning capabilities of the prototype. To avoid shorting the varactor and to prevent RF interaction between the bias lines and the antenna, two 10-MΩ resistors were soldered at the edge of the ground plane and pixelated patch. The single pixel connecting the ground plane to the optimized pixelated patch was replaced with a 100-pF capacitor to achieve dc isolation.

The capacitance of the varactor was varied from 2.8 to 0.3 pF by changing the bias voltage from 2 to 29 V. Due to the nonlinear behavior of the varactor diode, a much larger capacitance is expected when the bias voltage drops below 2 V. The reflection coefficients were measured in the band 1.6–4.6 GHz using an Agilent E5071C network analyzer; these are shown in Fig. 4. It is seen that, as the simulations predicted, decreasing the capacitance of the varactor diode shifts both resonances of the antenna upward. However, for higher values of capacitance, the return loss of the lower resonance is significantly smaller than predicted, limiting the tuning range of the lower resonance. In contrast, the tuning range of the upper resonance is somewhat larger than predicted, with a lower resonance frequency than predicted. The predicted behavior of the antenna can be improved with a better simulation model that includes the parasitic effects of the wires and components, and the nonlinearity and parasitics of the varactor, but the additional computational burden will be significant. Since the performance of the antenna when placed into a practical environment (such as embedded in a chip) will be significantly different than that of the prototype, use of a simplified model serves the purpose of demonstrating the validity of the proposed design approach. The frequency of resonance, as determined by maximum return loss, and the −10-dB bandwidth of the prototype for different bias voltages (and corresponding varactor capacitances) are provided in Table I.

The radiation patterns and efficiencies of the prototype antenna were measured for various bias voltages using a SATIMO near-field measurement system. The efficiencies are shown in Table I. Note that the frequency of maximum efficiency may be slightly different than the frequency of maximum return loss. It is observed that in the lower band, the radiation efficiency increases with increasing frequency, with a maximum efficiency of 42% achieved with a biasing voltage of 29 V. In the

Authorized licensed use limited to: JAMES MALONEY. Downloaded on February 19,2026 at 15:48:23 UTC from IEEE Xplore. Restrictions apply.

TABLE I
FREQUENCY OF RESONANCE AND −10-dB BANDWIDTH OF THE PROTOTYPE ANTENNA FOR VARIOUS VARACTOR CAPACITANCES

First Resonance				
Cap (pF)	Freq (GHz)	$\lvert S_{11} \rvert$ (dB)	BW (%)	Efficiency (%)
0.78/7V	2.31	-11.02	1.21	17
0.68/9V	2.38	-13.49	2.6	28
0.6/11V	2.44	-15.32	3.23	32
0.54/13V	2.47	-17.54	3.4	33
0.4/15V	2.53	-19.97	3.77	35
0.3/29V	2.58	-24.36	4.3	42
Second Resonance				
5/1V	3.1	-22.63	3.94	39
1.25/5V	3.31	-22.86	3.77	22
0.68/9V	3.58	-28.41	3.13	18
0.54/13V	3.84	-17.58	3.65	25
0.42/19V	4.156	-12.2	1.01	17

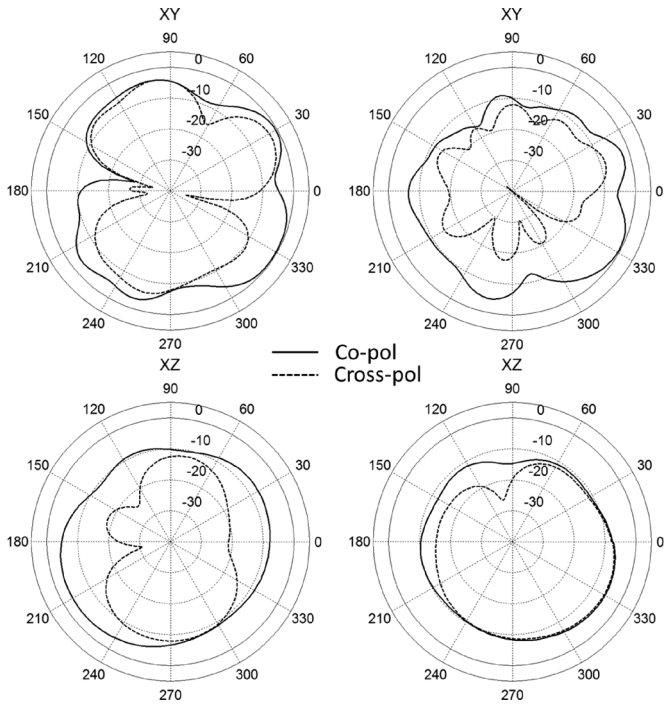

Fig. 5. Measured radiation patterns at *(left)* 2.4 and *(right)* 3.4 GHz.

upper band, the radiation efficiency decreases as the frequency increases, with a maximum efficiency of 46% achieved at 2.95 GHz when no biasing voltage is applied. The measured efficiencies are less than the simulation results, again due to the simplified biasing circuit and the ideal circuit model of the components used in the simulations. However, this antenna produces an efficiency similar to other tunable compact antennas, such as [12] and [13], but with a much smaller size. The measured realized gain patterns are plotted in Fig. 5, for both copolarization and cross-polarization, and in both the xy- and xz-planes of Fig. 1, at the two widely used frequency ranges for wireless communication: 2.4 and 3.4 GHz with biasing voltage of 13 and 7 V, respectively. The maximum gain does not, however, occur in these planes. At 2.4 GHz, the maximum realized gain is 2.37 dB, while at 3.4 GHz, it is −0.41 dB.

V. CONCLUSION

A design methodology for producing miniaturized and tunable planar antennas suitable for compact wireless applications has been demonstrated. By optimizing the geometry of a pixelated patch surrounding a monopole antenna, it has been shown that a high level of miniaturization can be achieved without the use of high-permittivity dielectrics. By varying the voltage of a properly chosen varactor diode, biased by a simple circuit that is integrated into the antenna structure, the resonance frequency of the miniaturized antenna can be continuously tuned within the ranges of 2.2–2.6 and 3–4.2 GHz while maintaining an acceptable impedance match and radiation efficiency.

REFERENCES

[1] C. A. Balanis, *Antenna Theory*, 3rd ed. Hoboken, NJ, USA: Wiley, 2005.
[2] T. J. Warnagiris and T. J. Minardo, "Performance of a meandered line as an electrically small transmitting antenna," *IEEE Trans. Antennas Propag. Mag.*, vol. 46, no. 12, pp. 1797–1801, Dec. 1998.
[3] J. P. Gianvittorio and Y. Rahmat-Samii, "Fractal antennas: A novel antenna miniaturization technique, applications," *IEEE Antennas Propag. Mag.*, vol. 44, no. 1, pp. 20–36, Feb. 2002.
[4] C. A. Balanis, *Modern Antenna Handbook*. Hoboken, NJ, USA: Wiley, 2008.
[5] Y. P. Zhang, "Finite-difference time-domain analysis of integrated ceramic ball grid array package antenna for highly integrated wireless transceivers," *IEEE Trans. Antennas Propag.*, vol. 52, no. 2, pp. 435–442, Feb. 2004.
[6] P. M. Mendes, A. Polyakov, M. Bartek, J. N. Burghartz, and J. H. Correia, "Design of a folded-patch chip-size antenna for short-range communications," in *Proc. 33rd Eur. Microw. Conf.*, 2003, pp. 723–726.
[7] R. O. Ouedraogo *et al.*, "In situ optimization of metamaterial-inspired loop antennas," *IEEE Antennas Wireless Propag. Lett.*, vol. 9, pp. 75–78, 2010.
[8] L. Greetis, R. O. Ouedraogo, B. Greetis, and E. J. Rothwell, "A self-structuring patch antenna: Simulation and prototype," *IEEE Antennas Propag. Mag.*, vol. 52, no. 1, pp. 114–123, Feb. 2010.
[9] J. Kovitz and Y. Rahmat-Samii, "Micro-actuated pixel patch antenna design using particle swarm optimization," in *IEEE Int. Symp. Antennas Propag. URSI Radio Sci. Meeting Dig.*, 2011, pp. 2415–2418.
[10] B. R. Holland, R. Ramadoss, S. Pandey, and P. Agrawal, "Tunable coplanar patch antenna using varactor," *Electron. Lett.*, vol. 42, no. 6, pp. 319–321, 2006.
[11] M. Maddela, R. Ramadoss, and R. Lempkowski, "PCB MEMS-based tunable coplanar patch antenna," in *Proc. IEEE Int. Symp. Ind. Electron.*, 2007, pp. 3255–3260.
[12] Z. J. Jin, J. H. Lim, and T. Y. Yun, "Frequency reconfigurable multiple-input multiple-output antenna with high isolation," *Microw., Antennas Propag.*, vol. 6, no. 10, p. 10951101, Jul. 2012.
[13] X. L. Sun, S. W. Cheung, and T. I. Yuk, "Dual-band monopole antenna with frequency-tunable feature for WiMAX applications," *IEEE Antennas Wireless Propag. Lett.*, vol. 7, pp. 569–572, 2008.
[14] V. A. Nguyen, M. T. Dao, Y. T. Lim, and S. O. Park, "A compact tunable internal antenna for personal communication handsets," *IEEE Antennas Wireless Propag. Lett.*, vol. 12, pp. 100–103, 2013.

Authorized licensed use limited to: JAMES MALONEY. Downloaded on February 19,2026 at 15:48:23 UTC from IEEE Xplore. Restrictions apply.